Exact Electron-Gas Response Functions at High Density

David C. Langreth
Serin Physics Laboratory, Rutgers University, Piscataway, New Jersey 08854

and

S. H. Vosko
Serin Physics Laboratory, Rutgers University, Piscataway, New Jersey 08854, and Department of Physics, University of Toronto, Toronto, Ontario, Canada M5S 1A7[a]
(Received 3 April 1987)

We calculate the Hohenberg-Kohn-Sham energy response kernel $K_{xc}(q)$ exactly for the high-density electron gas, and thus generalize the classic work of Ma and Brueckner to finite wave vector. The results are relevant to (1) density-functional theory, where we verify that one of the key assumptions used in the Langreth-Mehl functional was qualitatively correct and suggest possible improvements; (2) dielectric response theory, where we exactly calculate the leading correction to the static Lindhard screening function; and (3) a static attractive $1/r^6$-like interaction between like-charged point particles—we verify the recent suggestion of Maggs and Ashcroft that such an interaction exists and calculate its value.

PACS numbers: 71.10.+x

Here we present the results of a calculation of the Hohenberg-Kohn-Sham[1,2] energy response kernel $K_{xc}(q)$ of a dense electron gas. We begin with some definitions. Consider an electron gas of density $n(\mathbf{r})$ given by

$$n(\mathbf{r}) = n_0 + \sum_q \delta n_{\mathbf{q}} e^{i\mathbf{q}\cdot\mathbf{r}}, \tag{1}$$

where $\delta n_{\mathbf{q}}$ is taken to be small. The change in the exchange-correlation energy δE_{xc} associated with $\delta n_{\mathbf{q}}$ is

$$\delta E_{xc} = \sum_q K_{xc}(q) |\delta n_{\mathbf{q}}|^2, \tag{2}$$

thus defining K_{xc}. (We have chosen to follow the definition of K_{xc} in Ref. 1, which was also used in the work of Langreth and Perdew,[3] another commonly used definition differs by a factor of 2.) This quantity is also related to the dielectric function $\epsilon(q)$ of the electron gas by

$$\epsilon(q) = 1 - (4\pi e^2/q^2)\chi(q), \tag{3a}$$

$$\chi(q) = \chi_0(q)/[1 - 2K_{xc}(q)\chi_0(q)], \tag{3b}$$

where $\chi_0(q)$ is the free-electron density response function. Approximation of Eqs. (3) by setting K_{xc} equal to zero corresponds to the random-phase approximation, which is exact in the high-density limit; what we do here is to provide the leading correction.

The $q=0$ component of $K_{xc}(q)$ corresponds to the so-called local-density approximation for the energy. It is already known[4] to the order of the present calculation, and is larger than the nonlocal or $q\neq 0$ terms that we calculate here; so it is convenient to make the separation

$$K_{xc}(q) = K_{xc}(0) + \frac{\pi e^2}{8k_F^4} Z(q) q^2; \tag{4}$$

thus defining the dimensionless quantity $Z(q)$. To the order of our calculation $K_{xc}(0)$ is given by

$$K_{xc}(0) = -\frac{\pi e^2}{2k_F^2}[1 + \lambda(1 - \ln 2)], \tag{5}$$

where r_s is the usual electron density parameter, and

$$\lambda = (\pi a_0 k_F)^{-1} = 0.521 r_s/\pi = (k_{FT}/2k_F)^2.$$

The perturbation theoretic diagrams that contribute to $\chi - \chi_0$ to leading order in r_s have been known for years,[5,6] and are shown in Fig. 1. They were first evalu-

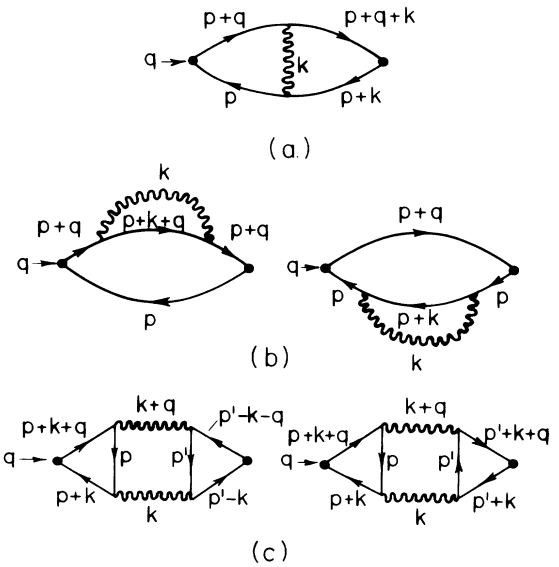

FIG. 1. Diagrams for the leading corrections to χ. At high densities they may be regarded as diagrams for $K_{xc}\chi_0^2$. The wiggly lines represent random-phase-approximation screened Coulomb interactions.

ated to order q^2 by Ma and Brueckner,[6] who proved the remarkable result that $Z(0)$ was a number independent of e^2 in the high-density limit, and when combined with the result of Sham[7] for exchange, one finds that $Z(0)=1.98-\frac{7}{9}$ at high densities. We note that any effects of the recent controversy[8] about whether the $\frac{7}{9}$ coefficient is correct because of long-range interactions without screening, cancel out of the net $Z(0)$ defined above. We emphasize that all diagrams in Fig. 1 make contributions of the same order to $Z(q)$ although the fluctuation diagram c makes numerically larger contribution to $Z(0)$ as first pointed out by Rasolt and Geldart[9]; we find here that the same thing happens at finite q, although diagrams (a) and (b) are now somewhat more important.

A wave-vector decomposition of these diagrams as a function of the k going through a Coulomb line was made for $Z(0)$ by Langreth and Perdew[3] as an aid to making an educated prediction as to how $Z(q)$ would behave. Langreth and Mehl[10] parametrized this prediction to produce a density functional, which is reasonably easily implementable in practice, and which has been applied with moderate success to atoms, molecules, bulk metals, and semiconductors. The physics behind these results, and especially the reason for the great importance of the fluctuation diagram, Fig. 1(c), in terms of plasmon exchange, has also been given.[11]

Here we evaluate $Z(q)$ exactly at high densities, and hence generalize Ma and Brueckner's calculation[6] to finite q. It would, of course, be nice to be able to relax this high-density restriction. In this regard we make the following comments. First, the anomalously large correlation contribution occurs only at very small q (scaling with the Fermi-Thomas wave vector k_{FT}), and our results should be meaningful until the density becomes so low that this region becomes comparable in size to the Fermi diameter. This was indeed our experience previously[3] where our results at $r_s=2$ or so were virtually identical to those at $r_s\simeq 0$. It was also found that contributions from higher-order diagrams[12] gave considerably larger corrections than the correction obtained by evaluating the diagrams of Fig. 1 at metallic densities as opposed to $r_s\simeq 0$. Next, we mention that the diagrams of Fig. 1 each have nonintegrable divergences as the intermediate wave vector k crosses the Fermi diameter[8,9]; when all the diagrams are summed, these divergences degenerate into a very rapidly varying but integrable structure whose strength increases with r_s. Because the net effect of this structure was found to be very weak,[3] the amount of analytic and numerical work necessary to integrate over it was in retrospect way out of proportion to any benefit gained. We therefore decided in this work to eliminate the problem by evaluating the diagrams of Fig. 1 at high density.

The procedure for taking the high-density limit of the diagrams of Fig. 1 is straightforward. First, make the separation

$$Z(q)=Z_c(q)+Z_x(q), \tag{6}$$

where $Z_x(q)$ is the value of Figs. 1(a) and 1(b) evaluated with bare instead of screened Coulomb lines. If necessary, use Sham's method[7] to resolve any $k\simeq 0$ anomolies, since such anomolies,[8] if they exist, must cancel out of the sum in Eq. (6), so that we may take $Z_x(0)$ equal to Sham's value of $-\frac{7}{9}$ (in the present units). To calculate $Z_c(q)$ we simply scale q and k in the diagrams in units of k_{FT} (we chose $k_{FT}/\sqrt{3}$ in view of our previous experience) and then expand in powers of this parameter divided by the Fermi diameter $2k_F$. This procedure would fail if it turned out that the main contribution was not concentrated in a small region in k and q space (of size $\sim k_{FT}/\sqrt{3}$) about the origin, but we, in fact, expect such a concentration at small q, and indeed this is how it turns out. If it were otherwise it would mean that the correlation energy associated with a localized disturbance was of the same order in e^2 as the exchange energy; such a situation could at best be described as counterintuitive. At high densities, and in the region where $Z_c(q)$ makes an important contribution, $Z_x(q)$ does not vary, because there is no possibility for the wave-vector scale k_{FT} to occur. Therefore over the scale of the plots shown in this paper, one may simply take $Z_x(q)$ to be its zero q value of $-\frac{7}{9}$. For larger q's, it may be taken from existing calculations.[8,13] Note that for larger q's, $Z(q)$ is dominated by $Z_x(q)$.

We now turn to the results for Z_c. First, consider the intermediate quantity $z_c(q,k)$ for which the summation over k in Fig. 1 has not been performed. This corresponds to the wave-vector decomposition of Langreth and Perdew.[3,14] We show curves in Fig. 2 for a variety of q values, and also the so-called gradient approximation curve (which corresponds to $q=0$) along with the Langreth-Mehl[10] fit to the gradient approximation (dashed line). The reader should compare the curves shown here with Fig. 1(a) of Ref. 3 on which the Langreth-Mehl approximation to Z_c was based. Basically what was done was to take the dashed curve for $k\gtrsim q$ and zero otherwise. The calculated curves show that this procedure was qualitatively justified. They also provide an answer to questions raised about this procedure.[15]

Our calculated result for $Z_c(q)$ is shown in Fig. 3. As anticipated the value of $Z_c(q)$ falls off sharply from its $q=0$ value; the wave-vector scale on which this happens is $\omega_p/v_F=k_{FT}/\sqrt{3}$. Thus as anticipated, the bulk of the contribution to $Z_c(q)$ occurs for both k and q within a very small region about the origin. Referring to Fig. 2, one sees that by k or $q\sim k_{FT}/\sqrt{3}$, the contribution has fallen off to small fractions of their original values. We do not expect substantial deviations from these high-density results until the size of this region becomes comparable with the Fermi diameter, and hence we fully expect our calculation to be meaningful at metallic densi-

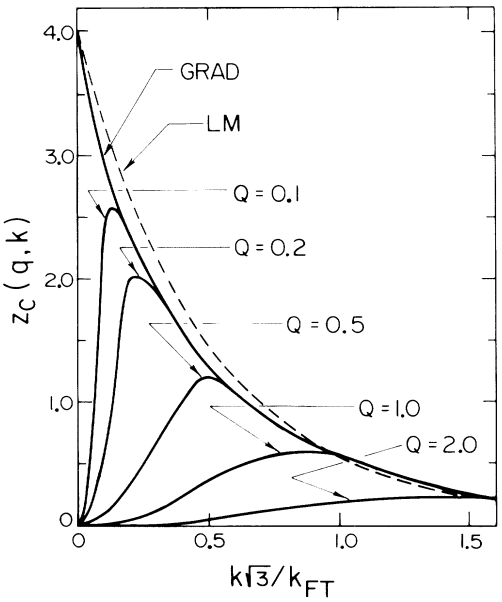

FIG. 2. Our calculations for the wave-vector decomposition $z_c(q,k)$ of $Z_c(q)$. These are shown (solid curves) for various values of Q, where $Q=q\sqrt{3}/k_{FT}$. The gradient approximation value is also shown. The dashed line is the fit of Langreth and Mehl with the gradient curve. The Langreth-Mehl approximation for the density functional consisted (in part) of cutting off this dashed curve for $k<k_c$, where $k_c\sim q$.

ties $r_s\sim 2$. As further evidence for this we have compared the curve marked GRAD in Fig. 2 with our earlier calculation[3] at $r_s=2$ and the results were almost identical.

Also shown for orientation in the dashed curves in Fig. 3 is the fitting function used by Langreth and Mehl[10] (LM),

$$Z_c^{LM}(q)=2\exp(-2k_c\sqrt{3}/k_{FT}), \tag{7}$$

for two different values of the cutoff parameter $k_c=q$ and $k_c=q/2$. Since in the LM scheme the value of k_c gets inextricably mixed with how q is approximated through ∇n when we extrapolate out of the linear response regime, one cannot say for sure which value of q_c more nearly corresponds to LM. One can say for sure, however, that the LM fitting function has the right qualitative behavior, except at large q where the correct Z_c falls off more slowly. However, in that region Z is dominated by Z_x. Use of the correct Z, however, rather than the approximation of Eq. (7) obviously allows one to improve the density functional, and this will be a subject of a future paper.

For small q, we find that $Z_c(q)$ behaves as

$$Z_c(q)\simeq 1.98+0.77Q\ln Q-1.25Q+\ldots, \tag{8}$$

where $Q=\sqrt{3}q/k_{FT}$. We found this to be fairly accurate (within 1%) for Q as large as 1 or so. Equation (8) plus

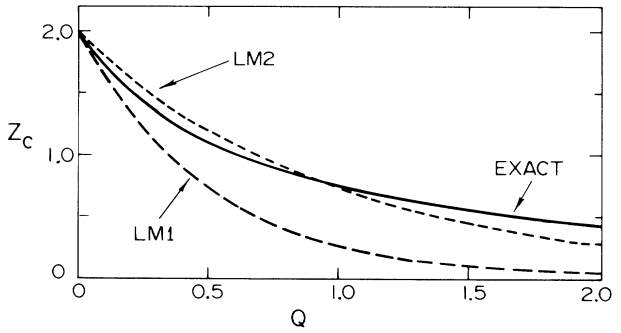

FIG. 3. Solid curve: The results of our exact calculations. Dashed curves: Eq. (7) for $k=q$ (LM1) and for $k=q/2$ (LM2). At $r_s=2$, the value of Q corresponding to the Fermi diameter is about 3.

Fig. 3 should be adequate for most applications of the response functions (3). A table of more accurate values will be included in a planned future paper. As mentioned earlier we expect the results to be useful at the higher metallic densities as well in the very high-density limit where they are rigorous.

One point which deserves emphasis is that $Z_c(q)$ falls away from its zero q value very rapidly, if q is measured on the more usual scale of $2k_F$, even at metallic densities. For example, for $Q=1$, $Z_c(q)$ is down to about half its zero q value and when $Q=2$, it is down to about $\frac{1}{4}$ of its zero q value. For reference, the value $Q\simeq 3$ corresponds to $q=2k_F$ at $r_s=2$. This means in particular that it is a bad approximation to use the $q=0$ result[6] at most physical q's.

After the bulk of this work was completed, we learned of work by Maggs and Ashcroft,[16] who on the basis of calculations involving diagram Fig. 1(c) predicted a power-law interaction at long range. Such an interaction, in the context of our work would be due to the nonanalytic behavior of $Z_c(q)$ near $q=0$ in Fig. 3(c). The second and third terms in (8) are not analytic functions of Q^2 about the origin. We find therefore[17] a tail in real space for large distances:

$$\frac{\delta V(r)}{V_{Coul}(r)}\simeq -\frac{1.31\lambda^2}{R^5}\ln(1.1R), \tag{9}$$

where $\delta V(r)$ is the extra interaction (in addition to the usual Friedel oscillations) between two point particles whose normal unscreened Coulomb interaction is $V_{Coul}(r)$ and $R=rk_{FT}/\sqrt{3}$. Notice that δV is attractive for like charges (and $R\gtrsim 1$) and scales as r^{-6} times a slowly varying coefficient. As pointed out previously,[3,11] the physical origin of the singularity giving rise to this peculiar behavior, is that plasmons scatter strongly off slowly varying disturbances whose length scales match their own (i.e., $k\lesssim\omega_p/v_F$) but weakly off more rapidly varying disturbances. Plasmons being unscreened can and in this case do mediate a long-range interaction.

We have considered here the interaction of nonelectronic particles. It is difficult to see, however, how the necessary additional vertex corrections to describe the electron-electron interaction could reduce the range or change the sign of the interaction of Eq. (9).

This work was supported in part by the National Science Foundation Grant No. DMR-83-04210 and by the National Sciences and Engineering Research Council of Canada Grant No. A6294. The computations were supported by the National Allocation Committee of the John von Neumann Center.

---

[a]Permanent address.

[1]P. Hohenberg and W. Kohn, Phys. Rev. **136**, B864 (1964).

[2]W. Kohn and L. D. Sham, Phys. Rev. **140**, A1133 (1965).

[3]D. C. Langreth and J. P. Perdew, Solid State Commun. **31**, 567 (1979), and Phys. Rev. **21**, 5469 (1980).

[4]M. Gell-Mann and K. A. Brueckner, Phys. Rev. **106**, 364 (1957).

[5]D. J. W. Geldart and S. H. Vosko, Can. J. Phys. **44**, 2137 (1966).

[6]S.-k. Ma and K. A. Brueckner, Phys. Rev. **165**, 18 (1968).

[7]L. J. Sham, in *Computational Methods in Band Theory,* edited by P. M. Marcus, J. F. Janak, and A. R. Williams (Plenum, New York, 1971).

[8]L. Kleinman, Phys. Rev. B **30**, 2223 (1984); P. R. Antoniewicz and L. Kleinman, Phys. Rev. B **31**, 6779 (1985).

[9]M. Rasolt and D. J. W. Geldart, Phys. Rev. Lett. **35**, 1234 (1975), and Phys. Rev. **13**, 1477 (1976).

[10]D. C. Langreth and M. J. Mehl, Phys. Rev. Lett. **47**, 446 (1981), and Phys. Rev. B **28**, 1809 (1983), and **29**, 2310(E) (1984).

[11]D. C. Langreth, in *Proceedings of the A. J. Coleman Symposium, 1985,* edited by R. Ehrdal and V. Smith (Riedel, Dordrecht, 1987).

[12]C. D. Hu and D. C. Langreth, Phys. Rev. B **33**, 943 (1986).

[13]D. J. W. Geldart and R. Taylor, Can. J. Phys. **48**, 155 (1970).

[14]We have not included the factor in Eq. (2.47) of the Phys. Rev. article in Ref. 3 as it was found there that its effect was fairly small. Its inclusion would result in small changes in Fig. 2 and *no* effect on Fig. 3 of the current paper. Its only use is to ensure that k is *precisely* the wave vector of the dynamic structure factor.

[15]M. Rasolt and D. J. W. Geldart, Phys. Rev. B **34**, 1325 (1986).

[16]A. C. Maggs and N. W. Ashcroft, Phys. Rev. Lett. **59**, 113 (1987).

[17]M. J. Lighthill, *Introduction to Fourier Analysis and Generalized Functions* (Cambridge, London, 1958), p. 43.